South African Journal of Chemical Engineering 35 (2021) 44–52

Contents lists available at ScienceDirect

South African Journal of Chemical Engineering

journal homepage: www.elsevier.com/locate/sajce

Editorial

Understanding the behavioral trends of the effect of water salinity and sand size on oil recovery in sandstone reservoirs

Emeka Emmanuel Okoro [a,*], Abdul-kabir Oluwaseyi Lawal [a], Kale B. Orodu [a], Samuel E. Sanni [b], Moses E. Emetere [c]

[a] Petroleum Engineering Department, Covenant University Ota, Nigeria
[b] Chemical Engineering Department, Covenant University Ota, Nigeria
[c] Physics Department, Covenant University Ota, Nigeria

ARTICLE INFO

Keywords:
Behavioral trend, grain size
Oil recovery
Sandstone reservoir
Water salinity

ABSTRACT

Enhanced oil recovery techniques are deployed to subsequently improve oil production having already employed primary or secondary recovery techniques or both methods simultaneously. Literature have shown that salinity impacts on oil recovery due to wettability alteration, but grain size which is closely related to the mechanical behavior and petrographical properties is also one of the main parameters controlling the phenomenon. There is need to investigate the effect of these two parameters in oil recovery. This study considered the effects of water salinity in the range of 0 to 20,000 ppm and sand grains of 45 to 300 μm on oil recovery. Flooding experiments and statistical analyses of the designed experiment was used to determine the residual oil saturation. The properties of sand samples such as bulk and pore volumes, porosity as well as, wet and dry weight for the various groups were also analyzed. Gauss-Newton algorithm with Levenberg-Marquardt modifications were the numerical scheme executed in MATLAB to formulate residual oil saturation model. The optimum percentage recovery for the core flooding experiment in each groups are 82.4%, 81.1%, 79.4%, 81.1% and 78.8% for A4, B4, C4, D4 and E5 respectively. Based on the experimental results, the 300 μm sand grains and salt concentration of 15,000 ppm should be used for operations in this reservoirs because, those conditions guarantee oil recovery as high as 82%. High oil recoveries correspond to low residual oil saturation and vice-versa. The recovered residual oil percentage had no direct correlations with the net dry and wet weights of the samples. The 45-micron grains had the least pore volume and it was observed that the percentage recoveries had no direct correlations with the core sample weights. During validation of the formulated residual oil saturation model, the model gave a good prediction of the experimental data within the 95% confidence interval, and from the statistical analyses, residual oil saturation decreased with decrease in water salinity. Thus, the larger the size of a grain, the lower its superficial area exposed to the wetting and non-wetting fluids which subsequently impacts on oil recovery.

1. Introduction

The aim of deploying oil recovery techniques is to produce hydrocarbons that will not flow naturally from the reservoir to the wellbore. These residual hydrocarbons are produced with the aid of advanced techniques known as enhanced oil recovery, which help to improve the economic lives of the reservoirs (Olabode et al., 2019). According to (Sakthhivel et al., 2017) chemical enhanced oil recovery (EOR) is one of the effective methods for recovering hydrocarbons from reservoirs. This technique primarily takes advantage of the oil-interfacial tension and injected fluids. According to Bera et al. (2011), the additives used in chemical EOR tend to reduce the interfacial tension which then improve the capillary forces within the reservoir pore spaces and thus, enhance the mobilization of the residual oil in the reservoir. Residual oil is the quantity of remaining oil in a depleted reservoir. The efficient operation of an enhanced oil recovery technique requires the development of a method that can increase the displacement efficiency in the already swept zones of the reservoir during primary or secondary oil recovery (Orodu and Tang, 2014; Johnw et al., 2017).

To improve oil recovery by water flooding, it is essential that the role played by interfacial forces in the entrapment of residual oil be studied and understood. Interfacial phenomena in natural rock, connate water

* Corresponding author:
E-mail address: emeka.okoro@covenantuniversity.edu.ng (E.E. Okoro).

https://doi.org/10.1016/j.sajce.2020.11.005
Received 2 January 2019; Received in revised form 10 September 2020; Accepted 15 November 2020
Available online 20 November 2020

and crude oil systems are very complicated because of the complexity of the natural liquids found in hydrocarbon reservoirs. Numerous studies of the displacement of oil by water under different interfacial tension or wettability conditions have been made (Soares and Thompson, 2009). For this immiscible liquid-liquid displacement (water flooding), non-wetting oil is pushed through the irregular void geometry of the porous medium. The displacement under these conditions is characterized by the movement of the oil followed by the mixed flow of the two streams (wetting and non-wetting oil streams). Darcy's law is satisfactory in the bulk of the porous medium at sufficiently low velocities but it fails to account for the effect of inertial terms, which become significant at high velocities (Freitas et al., 2011). The immiscible displacement of fluids in porous media is considered to include this non-Darcy effect, i.e. the effect of inertial terms also.

With the immiscible displacement process, the value of residual oil saturation is dependent on the vertical and horizontal sweep efficiencies, heterogeneity of the geological system as well as, the microscopic displacement efficiency. Microscopic displacement efficiency is not only dependent upon capillary forces but also on viscous and gravitational forces. At the initial stages of water flooding in a water wet reservoir, brine is found in the form of a film around sand grains, while the oil fills the remaining reservoir pore spaces (Orodu et al., 2018; Okoro et al., 2019). Al-Saedi et al. (2019) focused on the significance of reservoir chemical heterogeneity on EOR in sandstone reservoirs whereas, the impact of the sand grains sizes was not considered. Also, the study conducted by Teklu et al. (2012) only identified reservoir lithology and fluid properties as the main influential parameters during enhanced oil recovery screening.

Literature have shown that salinity impacts on oil recovery due to wettability alteration, but grain size which is closely related to the mechanical behavior and petrographical properties is also one of the main parameters controlling the phenomenon. There is need to investigate the effect of these two parameters in oil recovery. Thus, this study investigates the combined role of grain size and water salinity impact on residual oil recovery during water flooding for enhanced oil recovery in sandstone reservoirs. The properties of the sand samples such as bulk and pore volumes, porosity as well as, wet and dry weight for the various groups were analyzed. A very large fraction of the field tests of enhanced recovery projects have been failures because thy recovered less oil than had been projected. The most common reason for failure was the geological factors which resulted in poor sweep efficiency. Porosity is one of the geological factors in enhanced oil recovery, it impact was also considered.

2. Empirical review

Yan-Fei et al. (2010) discussed "Residual Volatilization of Oil in Homogeneous Porous Media" where the effects of pore size on residual oil and oil volatilization in a porous medium was investigated and simulated. The results showed that the maximum residual oil saturation in the medium decreased with an increase in the mean grain size. They asserted that the power function can be used to express the relationship between both parameters. The estimated volumetric retention per unit surface area was seen to increase with an increase in the mean grain size of the medium at a linear rate; this is due to the low grain surface area to volume ratio.

Ramez et al. (2011) carried out an experiment to investigate the efficiency of oil recovery during low salinity water flooding in sandstone reservoirs. In their work, secondary and tertiary core flooding experiments were run to determine the effect of water salinity on oil recovery. Deionized water and three different brines with concentrations ranging from 5000 to 174,000 mg/L were tested; these brine solutions were used to simulate the conditions in a Middle East field.

Shi et al. (2015) investigated the potential of spontaneous emulsification flooding for enhanced oil recovery in a high temperature and high salinity oil reservoir. In their work, emulsification tests and oil/water interfacial tension measurements were conducted in order to develop an alkali/surfactant emulsifier-system for quality separation of water and oil. The system is suitable for high-temperature and high-salinity Shengtuo reservoirs. Also, oil displacement efficiencies under different shear stresses were investigated using a sand pack flood test. The results showed that the interfacial tension of oil/water could be lowered to an ultra-low level by a synergistic effect of the alkali and surfactant which may subsequently give rise to the spontaneous emulsification of oil in brine within the porous medium.

Barnaji et al. (2016) investigated the effects of fine migration for enhanced oil recovery during low salinity flooding in sandstone cores. The experimental results showed that for both low salinity- and seawater- flooding, the migration of fines, did not in any way enhance oil recovery. Dang et al. (2016) in their study, provided detailed and extensive review of field applications of low salinity water flooding tecniques. Their research proposed a model for field-scale performance prediction and modeling of low salinity water flooding. They also highlighted the importance of capturing the effects of geology in low salinity water flooding processes.

(Yuan et al., 2017) investigated the role of Nanoparticles (NPs) in enhanced oil recovery process, it is believed that NPs fulfill the EOR purpose mainly through the mechanisms of interfacial tension (IFT) reduction and wettability alteration. They concluded that the applied nanoparticles (NPs) have super good disparity in the dispersant, the permeability reduction caused by NPs adsorption and straining was huge, and the adverse effects were worse at higher NPs concentrations.

Al-Saedi and Flori (2018) examined the effects of the chemical properties of salt-water and formation mineral composition on the water-rock interaction and its wettability. The measured wettability from the experimental results supports the proposed theory in their study. The core flooding results showed an ion exchange on the surface of quartz, while the clay mineral was found to have little effect on oil recovery.

3. Methodology

In this study, the experimental determination of the combined effects of grain size and water salinity on oil recovery was investigated. Sand flooding experiments were carried out using unconsolidated formation from the Niger Delta region. Five groups consisting of five samples each were prepared to effectively study the interactions of both selected parameters (grain size and salinity) during oil recovery. Each group was assigned a particular grain size while the prepared brine concentration was varied within a specified range. Sand grain sizes of 45 to 300 μm were used throughout this experiment. Sand properties such as bulk and pore volumes, porosity as well as, wet and dry weight for the various sample groups were analyzed.

The simplest direct method for determining bulk volume of a consolidated sample with a well-designed geometric shape is to measure its dimensions. The method is applicable to cylindrical cores with smooth-flat surfaces. The usual procedure is to determine the volume of fluid displaced by the sample. The fluid volume that the sample displaced was determined gravimetrically. Gravimetric determination of the bulk volume was accomplished by measuring the loss in weight of the samples when there were immersed in the fluid. The grain volume was determined from the dry sample weight and the grain density (Kashif et al., 2019). The pore volume was determined by measuring the effective porosity. The method is based on the intrusion of a fluid into the pore space of the sample. The pore volume was measured directly by resaturating the clean sandstone core sample with fluid. The porosity was then determined using the measured pore volume and bulk volume using Eq. (1).

$$Porosity = \frac{V_p}{V_b} \tag{1}$$

Where, V_p is the pore volume and V_b is the bulk volume.

3.1. Brine Preparation

5000,10,000,15,000 and 20,000 ppm brine solutions were prepared by dissolving 5,10,15 and 20 g of salt (NaCl) in 1000 mL of distilled water at ambient temperature (25 °C). The solution was stirred gently (20 rpm) for about 30 min and left to stand for 24 h in order to ensure that the salt was fully dissolved.

3.2. Flooding Procedure

Water flood provides a main driving mechanism to recover the residual oil, and gravity was used to improve sweep-out and oil recovery. This was achieved by injecting the fluid and producing the reservoir (represented by the core sample) at a rate low enough for gravity to keep the less dense solvent segregated from the crude oil and suppressing fingers of solvent as they try to form. The experimental setup of the flooding system is shown in Fig. 1. The schematic of the apparatus in Fig. 1 consists of accumulators for holding the fluids (brine or crude oil), a cylindrical tube with two end sterns housing the unconsolidated sand samples, flow lines with control valves, and a separator (separating funnel). Gravity is the only source of displacement, that is, the displacement velocity was sufficiently low, gravity would act to prevent the formation of fingers at the solvent/oil interface.

3.3. Flooding with crude oil

Crude oil was poured into the tank / accumulator and connected to the cylindrical tube in which flooding was stimulated and streamed via the flow lines, the flow control valve and end sterns. The crude oil was left to displace the brine in the sand sample until only crude oil began coming out of the core.

The volume of the displaced water in the funnel is equal to the volume of the crude oil in the sample sand; this is termed the hydrocarbon pore volume.

Determination of Connate Water Saturation:

$$S_{wc} = \frac{V_{wc}}{HCPV + V_{wc}} \tag{2}$$

where:

S_{wc} = connate water saturation
V_{wc} = connate water volume, cm^3
HCPV = hydrocarbon pore volume, cm^3

3.3.1. Flooding with brine

Prior to this experiment, a control experiment was conducted with non-saline water flowing through the set-up containing the different sand cores; this is so as to clearly perceive any effect of salt in crude oil/brine in contact with the sand particles afterwards. For each sand sample, the same concentration of brine used in saturating it, was poured into the accumulator and connected to the flooding tube to displace the crude oil. The control valve was opened and the displacement was observed until only water with oil traces seeped through the sand sample.

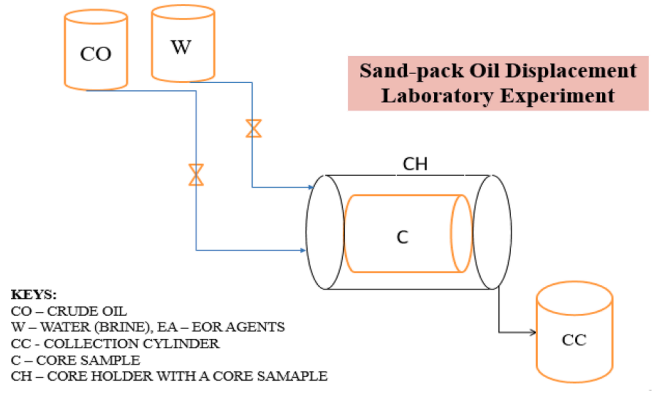

Fig. 1. Set up for the Vertical Core Flooding Experiment.

The core samples were first saturated with crude oil before commencing the core flooding experiments (Fig. 5). The first sand core samples of the groups (A1, B1, C1, D1 and E1) were used for water flooding alone (no salt was added), so as to observe the effect of non-salinity in oil recovery of the cores. The amount of brine used to displace the crude oil was ten times the pour volume of the sand sample and at that volume; it was observed that all recoverable crude oil in the sample had been made possible by the displacing fluid/brine. The recovered oil in the cylinder was then recorded.

Note: Recovered oil (N_P) = oil displaced by the brine = volume of oil in the cylinder

Estimation of Recovery Efficiency:

$$\%\text{Recovery Efficiency} = \frac{N_p}{HCPV} \times 100\% \tag{3}$$

where:

N_p = cumulative oil produced, cm^3

3.4. Modelling of residual oil saturation

It has been demonstrated through core flooding experiment that displacement in water injection process depend upon pore structure apart from all other factor. The bypassing of oil is due to microscopic heterogeneity resulting from non-uniform pores structure. Design of experiments was used to statistically model the residual oil saturation from the observed experimental results. This technique utilizes dynamic handling of experimental outcomes to enhance its presentation while screening less pertinent data. The experimental results were first presented as a conventional 'response surface methodology' (RSM) scheme. The RSM considered the residual oil saturation (S_{or}) as the model outcome while brine concentration (C_i), average grain size (d_G), and connate water saturation (S_{wc}) as the input variable factors.

$$S_{or} = \beta 0 + A + B + C \tag{4}$$

where,

$$A = (\beta 1 \times C_i) + (\beta 2 \times d_G) + (\beta 3 \times S_{wc}) \tag{5}$$

$$B = (\beta 4 \times C_i \times d_G) + (\beta 5 \times C_i \times S_{wc}) + (\beta 6 \times d_G \times S_{wc}) \tag{6}$$

$$C = (\beta 1 \times C_i^2) + (\beta 2 \times d_G^2) + (\beta 3 \times S_{wc}^2) \tag{7}$$

C_i = Salinity (ppm)
d_G = grainsize (μm)S_{wc} = Connate water saturation (%)

Iterative approach which has been seen as a robust approach in calculating the alpha factors was adopted, and it does not assume residual oil composition to be the same throughout the simulation (Bourgeois et al., 2011). The most noticeable point in the calculation is that the alpha factor theory is written in terms of hydrocarbon volume, rather than saturations, allowing a single value of alpha factor to be adaptable for different levels of water saturation. The coefficients β0, β1, β2, β3, β4, β5, β6, β7, β8, and β9 were estimated within the 95% confidence interval using a numerical scheme implemented by Gauss-Newton algorithm with Levenberg-Marquardt modifications. This numerical scheme was executed in MATLAB using the function 'nlinfit'. Adopting initial guess for the coefficients β0 through β9, the first estimated mathematical/linear model equations that were obtained are given as:

$$S_{or} = 30.5114 + A + B + C \tag{8}$$

$$A = -0.0001 \cdot C_i - 0.0167 \cdot d_G + 0.0169 \cdot S_{wcv} \quad (9)$$

$$B = 0.0000 \cdot C_i \cdot d_G + 0.0000 \cdot C_i \cdot S_{wc} - 0.0001 \cdot d_G \cdot S_{wc} \quad (10)$$

$$C = -0.0000 \cdot C_i^2 + 0.0000 \cdot d_G^2 + 0.0005 \cdot S_{wc}^2 \quad (11)$$

All coefficients with ±0.0000 were screened out and the program was rerun using a modified general mathematical model with the remaining values maintained as initial coefficient guesses.

4. Results and discussion

The outcomes obtained from the outlined experiments of the combined effects of sand grain size and water salinity on oil recovery are presented in this section. Flooding experiments and statistical analyses of the designed experiments were used to determine the residual oil saturation and thus, model its outcome respectively. The entire results portray a strong influence of both parameters on oil recovery.

Table 1 presents a summary of the sample groups and their corresponding grain sizes used to prepare the sand samples categorically. Each group was assigned a particular grain size while the prepared brine concentration was varied within a specified range. The selected grain sizes were obtained from laboratory sleeve analysis. Grain sizes of 45 μm to 300 μm were used throughout this experiment.

Concentration values of 0 to 20,000 ppm salt in water were applied in determining the porosity of sand samples at all stages of the experiment. Properties of the prepared sand samples were measured and evaluated with conventional techniques as discussed in section 3.0. All data recorded during the experiment are presented in Table 3.

4.1. Appraised sand properties for various samples

Table 3 shows the appraised Sand sample properties of the core samples used for core flooding experiment for each group. Table 3 and Figs. 2 through 4 present a summary of the appraised sand properties for various sample groups.

From Fig. 2, it was observed that group E has the lowest net dry and wet weights (which range from 86 to 91 gm) when compared to the other four groups (A, B, C, and D). Group B had the highest net dry and wet weights followed by group A (Fig. 2).

Fig. 3 shows that sample C has the least bulk volume followed by sample A. Also, sample A gave the least pore volume, hence in an increasing order of pore volume, the order is samples A, C, D, B and E (Fig. 3) while Fig. 4 shows the grouped samples with their corresponding porosities. John et al. (2017) highlighted the importance of these parameters in determining the porosity of the core samples. Gbadamosi et al. (2019) also noted the importance of the petro-physical property in influencing oil recovery. Thus, it is inexcusable to start an EOR project without obtaining as much information as possible on the shape, size and heterogeneity. The most common types of reservoir heterogeneity is simply variations in porosity and permeability in the reservoir formation samples. According to the study by Roldan-Carrillo et al. (2012), the reservoir porosity is one of the important variables for EOR operations and low porosity will limit the applicability of the EOR methods. Fig. 4 shows that core samples from group B to E have good porosity profile when compared to group A. This shows that groups B to E have more permeable layers. The heterogeneity of the core samples is more dominant than expected, and these attributes are commonly conferred on a sediment by the process of washing to remove the fine particles from the coarser ones, leaving pores that are big enough to permit oil to enter against the capillary forces which tend to exclude them. Sandstone has been reported in literature to had shown oil recoveries from 9 to 21% using displacement test (Alvarado and Manrique, 2010; Hatner et al., 2011).

Table 1
Grain Sizes of Sand Sample Groups.

Sand Sample Group	A	B	C	D	E
Grain Size (μm)	300	250	100	80	45

4.2. Flooding of core sand sample groups

The results show that sand sample A4 flooded with 15,000 ppm yielded the highest oil recovery of 82.4%. The first core sample of each group (A1, B1, C1, D1, and E1) with 300, 250, 100, 80, and 45 μm grain size respectively, recorded the least oil recovery when flooded with non-saline water (Fig. 6). All residual oil saturation values were calculated from the initial oil saturation value which is a function of the interstitial water saturation. It was observed that sample A4 with the highest oil recovery factor had the least residual oil saturation of 17.6% (Fig. 6). Fig. 6 shows that core sample B4 flooded with 15,000 ppm brine yielded 81.1% oil recovery; Core sample B1 recorded the least value of oil recovery factor (i.e. 71.4%) for group B, because it was flooded with non-saline water. All residual oil saturation values were calculated from the initial oil saturation. It was observed that sample B4 with the highest oil recovery for group B gave the least residual oil saturation of 18.9% (Fig. 5).

According to Dang et al. (2016), among the existing hypotheses in enhanced oil recovery, wettability alteration towards increased water wetness is the widely suggested case of increased oil recovery. Literature have also shown through experimental analysis that changes in the injected brine composition can improve water flood performance (Morrow et al., 2011; Drummond and Israelachvili, 2004; Loahardjo et al., 2010). The trends in crude oil recovery and recovery factors for Figs. 5 and 6 were in excellent agreement with literature. This concept is known as the optimal injection brine composition for water flood.

Fig. 7 shows the relationship between recovery factor, salinity and grain size. It was observed that the optimum recovery with respect to salinity was 15,000 ppm for the five (5) grain size samples under consideration. Group A with grain size of 300 μm had the highest recovery factor at the optimum salinity of 15,000 ppm; and was followed by groups D, B, C and E respectively. The salinity of the injected water is controlled to improve oil displacement efficiency. Austad et al. (2010) highlighted that brine flooding efficiency can be attributed to reduction in interfacial tension not generation of in-situ surfactant. This phenomenon can be physically explained by the ionic exchange between the injected brine and formation water. The ionic exchange during this process leads to the adsorption of divalent ions and changes in the ionic composition of formation water and the wettability condition (Fjelde et al., 2012).

Fig. 8 shows that core sample C4 flooded with 15,000 ppm yielded the highest oil recovery of 79.4% for the group. Core sample C2 recorded the least oil recovery of 71.8% when flooded with 5000 ppm saline water. All residual oil saturation values were calculated based on the initial oil-saturation. It was observed that sample C4 with the highest oil recovery had the least residual oil saturation of 20.6% in its group.

The crude oil recovered from Group 'D' core samples shows that core sample D4 flooded with 15,000 ppm yielded the highest oil recovery of 81.8%. Sand sample D1 recorded the least oil recovery of 70.6% when flooded with non-saline water. It was also observed that sample D4 had the least residual oil saturation of 18.2%.

The crude oil recovered from Group 'E' shows that sand sample E5 flooded with 20,000 ppm yielded the highest oil recovery of 78.8%. Sand sample E1 recorded the least oil recovery of 70.3% when flooded with non-saline water, while sample E4 gave the least residual oil saturation of 21.2%.

4.3. Statistical analysis of experimental design

A statistical model was used to determine the residual oil saturation from the observed experimental results. This technique adopts the

Table 2
Core Flooding Experimental Data for the Sand Sample Groups.

Core Sample	Grain Size (μm)	Salinity (ppm)	Core Sample	Grain Size (μm)	Salinity (ppm)	Core Sample	Grain Size (μm)	Salinity (ppm)
A1	300	0	B1	250	0	C1	100	0
A2	300	5000	B2	250	5000	C2	100	5000
A3	300	10,000	B3	250	10,000	C3	100	10,000
A4	300	15,000	B4	250	15,000	C4	100	15,000
A5	300	20,000	B5	250	20,000	C5	100	20,000
D1	80	0	E1	45	0			
D2	80	5000	E2	45	5000			
D3	80	10,000	E3	45	10,000			
D4	80	15,000	E4	45	15,000			
D5	80	20,000	E5	45	20,000			

Table 3
Appraised Sand Properties for Sand Sample Groups.

Sand Sample	Length, L (cm)	Sand Sample	Length, L (cm)	Diameter, D (cm)	Sand Sample	Length, L (cm)	Diameter, D (cm)
A1	5.94	B1	6.18	3.30	C1	6.13	3.30
A2	6.09	B2	6.22	3.30	C2	6.16	3.30
A3	6.06	B3	6.21	3.30	C3	6.00	3.30
A4	6.14	B4	6.12	3.30	C4	5.81	3.30
A5	6.14	B5	6.22	3.30	C5	6.17	3.30
D1	6.01	E1	6.08	3.30			
D2	6.21	E2	6.06	3.30			
D3	6.18	E3	6.24	3.30			
D4	6.16	E4	6.07	3.30			
D5	6.11	E5	5.98	3.30			

* The diameter is the same = 3.30 cm.

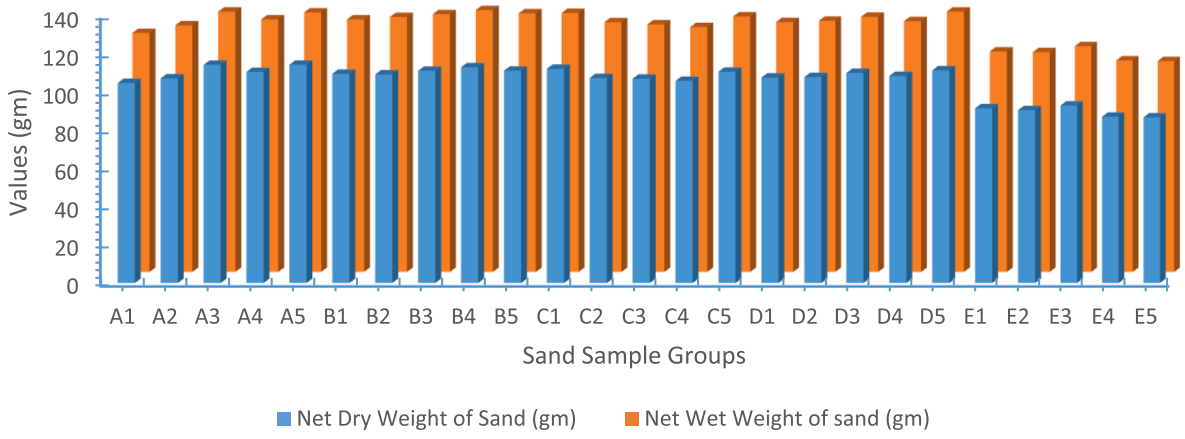

Fig. 2. Appraised Net Dry and Wet Weights for Sand Sample Groups.

dynamic technique in handling experimental outcomes in order to enhance its presentation while screening less pertinent data. The experimental results were first presented in a conventional 'response surface methodology' (RSM) scheme. The residual oil saturation (S_{or}) is the model outcome while brine concentration (C_i), average grain size (d_G), and connate water saturation (S_{wc}) are the input variables. Table 4 represents the results obtained from the RSM scheme/laboratory experiments.

In line with design of experiments, each input factor was considered at three levels denoted by high (+1), medium (0), and low (−1) values. This standard notation was used to represent the maximum, median, and minimum values of each input factor (C_i, d_G, and S_{wc}). The D-optimal design approach was then adopted to reorient the notations of each input factor in order to minimize the total number of experimental runs while eliminating irrelevant data. This program was executed in MATLAB using the function 'cordexch'. All the residual oil saturation values that fell outside the experimental results were calculated from similar recovery factor points. An implementation of this scheme is presented in Table 5.

The C_i values at the maximum, median and minimum points were identified as 20,000 ppm, 10,000 ppm and 0 ppm respectively. Experimental minimum, median and maximum values of d_G were 45, 100 and 300 μm respectively. Minimum S_{wc} of 15.4%, median of 25.8%, and maximum of 35.1% were identified. These values were used to replace the −1, 0, 1 notations before implementing the next stage. Prior to the next stage, a general multivariate nonlinear model of second order was generated for the input factors as 'independent variables', while the response factor (S_{or}) was taken as the 'dependent variable'.

Based on the regression analysis conducted using Eq. (11), an evaluation of the 'goodness of fit' was done from the obtained residuals. Fig. 9 shows the error bar plots of the formulated model about the augmented D-optimal design points. The generated error bar shows a range of deviations for the case number points analyzed. Consequently, Eq. (11) was then used to validate the experimental sand flood data about the general experimental points. Figs. 9 and 10 present a summary of the physical and mathematical models analyzed in this research.

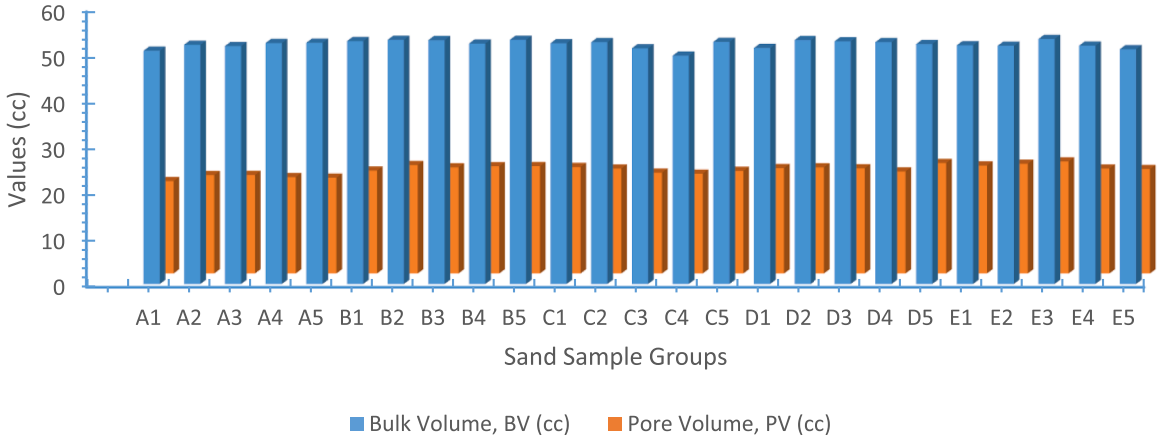

Fig. 3. Appraised Bulk and Pore Volume of Cores for Sand Sample Groups.

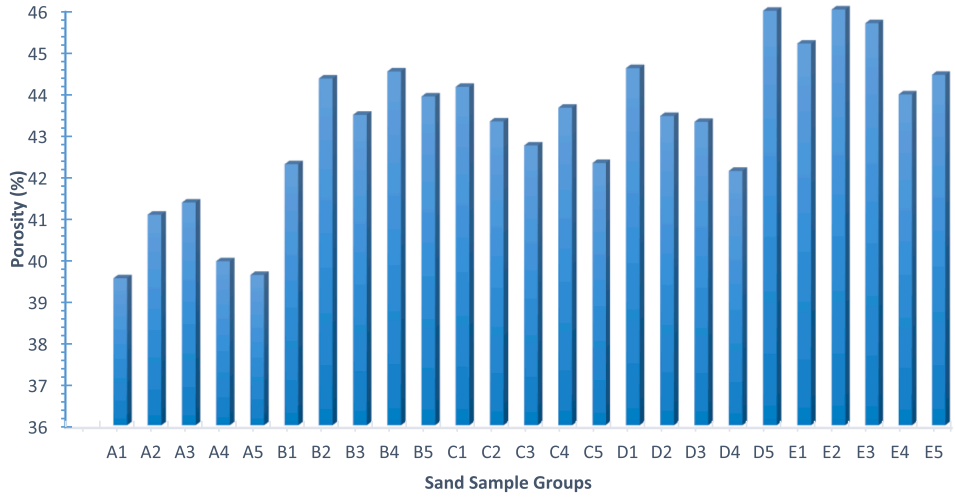

Fig. 4. Appraised Porosity of Cores for Sand Sample Groups.

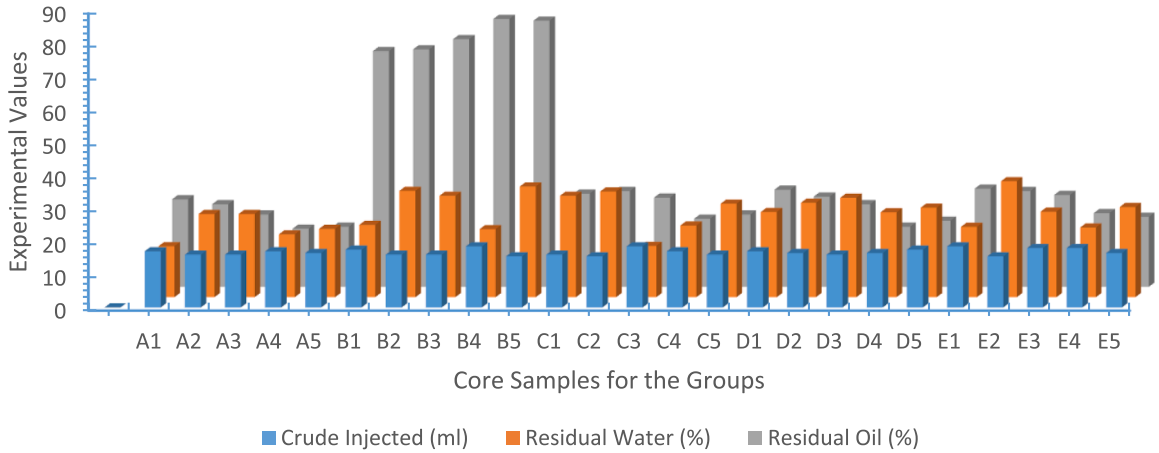

Fig. 5. Volume of Crude Oil injected, Residual Water and oil for the Core Samples.

The residual oil volume is a function of salinity, grain size and connate water saturation. Figs. 9 and 10 show that as the salinity concentration increases, the percentage residual oil saturation decreases. This increase was found to be caused by a decrease in the interfacial tension (IFT). This effect caused a reduction in capillary pressure, thus increasing the tendency to reduce the residual oil saturation. Reducing IFT increases the tendency of water to displace oil by decreasing the capillary forces.

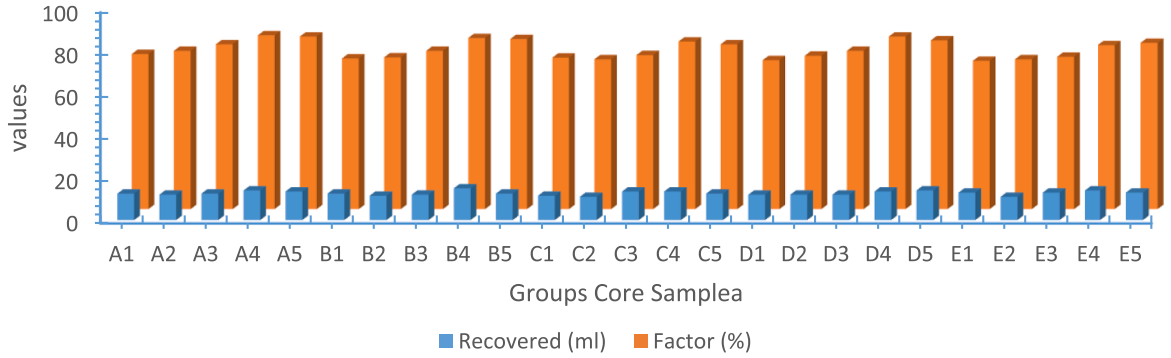

Fig. 6. Core Sample Recovery Factors and Volume of Crude Oil Recovered for the Core-Groups.

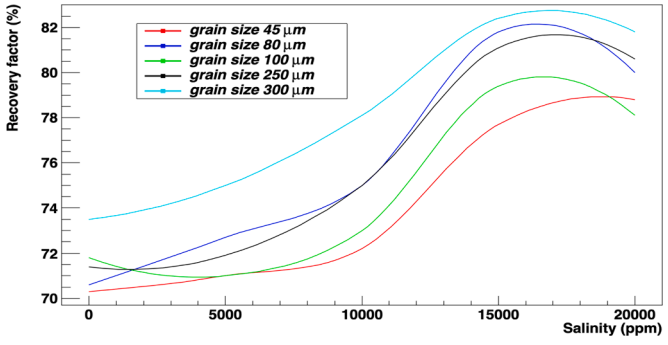

Fig. 7. Recovery Factor for Sand Sample Groups and differing Salinity.

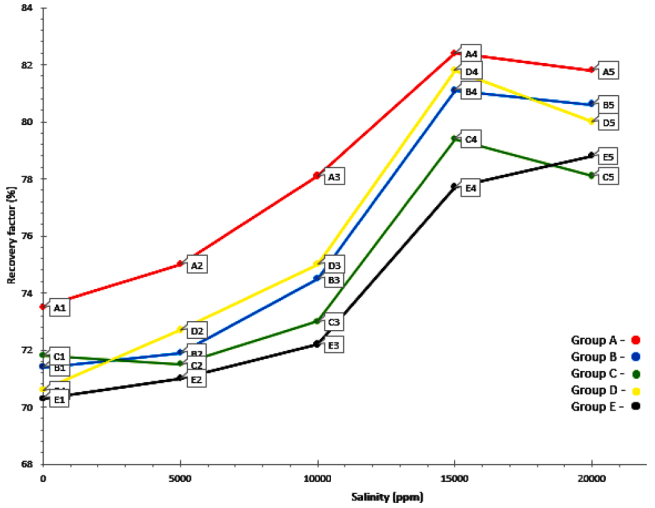

Fig. 8. Salinity impact on Recovery Factor for the Core Samples.

When a wetting and a non-wetting phase flow together in a reservoir rock, each phase flows along separate and distinct paths. The distribution of the two phases is according to their wetting characteristics which is also a function of their relative permeabilities through the rock. Since the wetting phase occupies the smaller pore openings at small saturations, and these pore openings do not contribute materially to flow, it follows that the presence of a small wetting phase saturation will affect the non-wetting phase permeation through the rock only to a limited extent as observed in Fig. 9 which do not span from the origin; in a water-oil system, oil is usually the non-wetting phase. This residual oil saturation model below was obtained as the terminal equation. A regression analysis was conducted on Eq. (12) in order to evaluate the

Table 4
Experimental Outcomes of the Response Surface Methodology Scheme.

Run No.	C_i (ppm)	d_G (μm)	S_{wc} (%)	S_{or} (%)
1	0	300	15.4	26.5
2	5000	300	25.2	25.0
3	10,000	300	25.2	21.9
4	15,000	300	19.0	17.6
5	20,000	300	20.7	18.2
6	0	250	21.9	28.6
7	5000	250	32.2	28.1
8	10,000	250	30.7	25.0
9	15,000	250	20.6	18.9
10	20,000	250	33.5	19.4
11	0	100	30.7	28.2
12	5000	100	32.0	29.0
13	10,000	100	15.5	27.0
14	15,000	100	21.7	20.6
15	20,000	100	28.3	21.9
16	0	80	25.8	29.4
17	5000	80	28.6	27.3
18	10,000	80	30.1	25.0
19	15,000	80	25.7	18.2
20	20,000	80	27.1	20.0
21	0	45	21.3	29.7
22	5000	45	35.1	29.0
23	10,000	45	25.9	27.8
24	15,000	45	21.1	22.3
25	20,000	45	27.3	21.2

Table 5
Optimal Design Scheme of Experimental Outcomes.

Runs	C_i	d_G	S_{wc}	S_{or}
1	−1	−1	−1	29.7
2	−1	1	−1	26.5
3	−1	1	1	26.5
4	1	−1	−1	21.2
5	1	1	−1	18.2
6	0	0	−1	27.0
7	1	−1	1	21.2
8	0	−1	0	27.8
9	1	1	1	18.2
10	−1	−1	1	29.7
11	0	1	1	21.9
12	−1	0	0	28.2

'goodness of fit' from the obtained residuals.

$$S_{or} = 28.3578 - 0.0004 \cdot C_i - 0.00155 \cdot d_G + 0.2473 \cdot S_{wc} + 0.0001 \cdot d_G \cdot S_{wc} - 0.0056 \cdot {S_{wc}}^2 \quad (12)$$

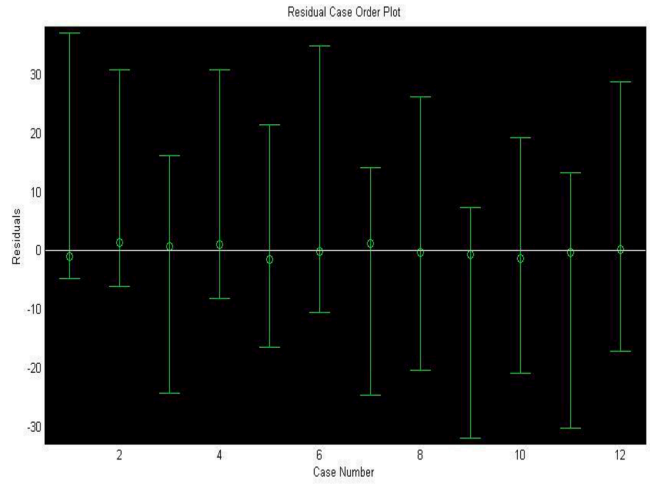

Fig. 9. Residual Case Order Plot.

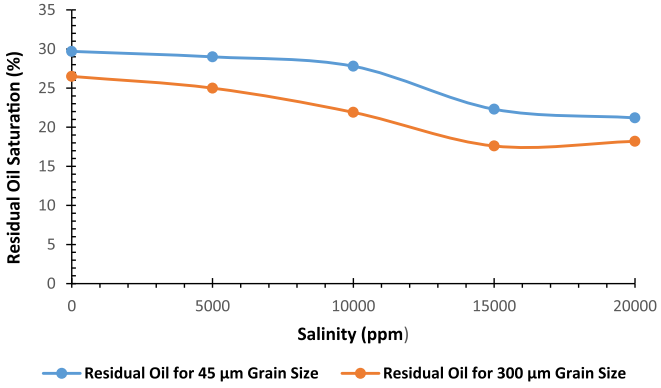

Fig. 10. Residual Oil-Salinity Variation for Grain Size.

5. Conclusion and recommendations

This study examined oil recovery with respect to grain size and salinity on a laboratory scale. The experimental results and modeling of the process were carried out in view of establishing a behavioral trend useful for forecasting residual oil saturation in the presence of limited data. Based on the findings of this study, the results obtained from the laboratory investigations show that oil recovery in the presence of brine concentration value of 15,000 ppm gave the highest recovery of 82%. It was also observed that the highest recovery was obtained for sand of 300 µm for brine concentration of 15,000 ppm. The residual oil saturation model formulated at a 95% confidence interval illustrated good predictability/validation of experimental data. From the observations made, the recommendations from this research are as follows: The input factors used in the engineering statistical analysis of designed experiments were limited to laboratory data from core flood experiments. To adopt the residual oil saturation model and improve its applicability, more input factors should be considered. This idea may foster extensive research considerations in the near-future. The developed concept as highlighted in this study, may also be incorporated in the engineering statistical models.

Declaration of Competing Interest

The authors declare that they have no known competing financial interests or personal relationships that could have appeared to influence the work reported in this paper.

Acknowledgement

The authors would like to thank Covenant University centre for Research Innovation and Discovery (CUCRID) Ota, Nigeria for its support in making the publication of this research possible.

References

Al-Saedi Hasan, N., Flori Ralph, E., 2018. Enhanced oil recovery of low salinity water flooding in sandstone and the role of clay. Petroleum Exploration and Development 45 (5), 927–931. https://doi.org/10.1016/S1876-3804(18)30096-X, 2018.

Alvarado, V., Manrique, E., 2010. Enhanced oil recovery: an update review. Energies 3, 1529–1575. https://doi.org/10.3390/en3091529.

Austad T., RezaeiDoust A., Puntervold T. (2010) Chemical mechanism of low salinity water flooding in sandstone reservoir. SPE-129767, In: SPE Improved Oil Recovery Symposium, Tulsa, 24–28 April.

Bera, A., Ojha, K., Mandal, A., Kumar, T., 2011. Interfacial tension and phase behaviour of surfactant-brine-oil system. Colloids Surfaces A 383, 114–119. https://doi.org/10.1016/j.colsurfa.2011.03.035.

Bourgeois M.J., Thibeau S., Guo J. (2011) Modelling residual oil saturation in miscible and immiscible gas floods by use of alpha-factors. SPE-143379-MS, In: SPE EUROPECEAGE Annual Conference and Exhibition, 23-26 May, Vienna, Austria. 10.2118/143379-MS.

Dang, C., Nghiem, L., Nguyen, N., Chen, Z., Nguyen, Q., 2016. Mechanistic modeling of low salinity water flooding. J Petroleum Science and Engineering 146, 191–209. https://doi.org/10.1016/j.petrol.2016.04.024.

Drummond, C., Israelachvili, J., 2004. Fundamental studies of crude oil-surface water interactions and its relationship to reservoir wettability. J Petroleum Science and Engineering 45, 61–68. https://doi.org/10.1016/j.petrol.2004.04.007.

Fjelde I., Asen S.V., Omekeh A. (2012) Low salinity water flooding experiments and interpretation by simulations. Paper SPE154142 presented at the Eighteenth SPE Improved Oil Recovery Symposium, Tulsa, OK, USA, April1 4–18.

Freitas, J.F., Soares, E.J., Thompson, R.L., 2011. Residual mass and flow regimes for the immiscible liquid–liquid displacement in a plane channel. Int J Multiphase Flow 37 (6), 640–646. https://doi.org/10.1016/j.ijmultiphaseflow.2011.03.003.

Gbadamosi, A.O., Junin, R., Manan, M.A., Agi, A., Yusuff, A.S., 2019. An overview of chemical enhanced oil recovery: recent advances and prospects. Int Nano Lett 9, 171–202. https://doi.org/10.1007/s40089-019-0272-8.

Al-Saedi, Hasan N., Brady, Patrick V., Flori, Ralph E., Heidari, Peyman, 2019. Insights into the role of clays in low salinity water flooding in sand columns. J Petroleum Science and Engineering 174, 291–305. https://doi.org/10.1016/j.petrol.2018.11.031.

John, M.F., Olabode, O., Egeonu, G., Ojo, T.I., 2017. Enhanced oil recovery of medium crude oil (310 Api) using nanoparticles and polymer. Int J Applied Engineering Research 12 (19), 8425–8435.

Kashif, M., Cao, Y., Yuan, G., Asif, M., Javed, K., Mendez, J.N., Khan, D., Miruo, L., 2019. Pore size distribution, their geometry and connectivity in deeply buried Paleogene Es1 sandstone reservoir, Nanpu Sag. East China. Pet. Sci. 16, 981–1000. https://doi.org/10.1007/s12182-019-00375-3.

Loahardjo, N., Xie, X., Morrow, N.R., 2010. Oil recovery by sequential water flooding of mixed-wet sandstone and limestone. Energy Fuels 24 (9), 5073–5080. https://doi.org/10.1021/ef100729b.

Barnaji, Milad Jafari, Pourafshary, Peyman, Rasaie, Mohammad Reza, 2016. Visual investigation of the effects of clay minerals on enhancement of oil recovery by low salinity water flooding. Fuel 184, 826–835. https://doi.org/10.1016/j.fuel.2016.07.076.

Morrow N.R., Buckley J.S. (2011) Improved oil recovery by low-salinity water flooding. JPT. Distinguished Author Series, pp. 106–112.

Okoro, E.E., Okoh, A., Ekeinde, E.B., Dosunmu, A., 2019. Reserve estimation using decline curve analysis for boundary-dominated flow dry gas wells. Arabian J Science and Engineering 44, 6195–6204. https://doi.org/10.1007/s13369-019-03749-2.

Olabode, O.A., Etim, E., Okoro, E., Ogunkunle, F.T., Abraham, V.D., 2019. Predicting Post breakthrough performance of Water and Gas Coning. Int J Mechanical Engineering and Technology 10 (2), 255–272.

Orodu, O.D., Orodu, K.B., Afolabi, R.O., Dafe, E.A., 2018. Dataset on experimental investigation of gum Arabic coating alumina nanoparticles for enhanced recovery of Nigerian medium crude oil. Data Brief 19, 475–480. https://doi.org/10.1016/j.dib.2018.05.046.

Orodu, O.D., Tang, Z., 2014. The performance of a high Paraffin reservoir under Non-isothermal water flooding. Pet Sci Technol 32 (3), 324–334. https://doi.org/10.1080/10916466.2011.565295.

Roldán-Carrillo, T., Castorena-Cortés, G., Reyes-Avila, J., Zapata-Peñasco, I., Olguín-Lora, P., 2012. Effect of porous media types on oil recovery by indigenous microorganisms from a Mexican oil field. J Chemical Technology & Biotechnology 88 (6), 1023–1029. https://doi.org/10.1002/jctb.3926.

Sakthivel, S., Velusamy, S., Nair, V.C., Sharma, T., Sangwai, J.S., 2017. Interfacial tension of crude oil-water system with imidazolium and lactam-based ionic liquids and their evaluation for enhanced oil recovery under high saline environment. Fuel 191, 239–250. https://doi.org/10.1016/j.fuel.2016.11.064.

Shi, S., Wang, Y., Wang, L., Jin, Y., Wang, T., Wang, J., 2015. Potential of Spontaneous Emulsification Flooding for Enhancing Oil Recovery in High-Temperature and High-Salinity Oil Reservoir. J Dispers Sci Technol 36 (5), 660–669. https://doi.org/10.1080/01932691.2014.905954.

Soares, E.J., Thompson, R.L., 2009. Flow regimes for the immiscible liquid–liquid displacement in capillary tubes with complete wetting of the displaced liquid. J Fluid Mech 641, 63. https://doi.org/10.1017/s0022112009991546.

Teklu T.W., Alameri W., Graves R.M., Tutuncu A.N., Kazemi H., Alsumaiti A.M. 2012. Geomechanics considerations in enhanced oil recovery. SPE-162701-MS, SPE Canadian Unconventional Resources Conference, 30 October – 1 November, Calgary, Alberta, Canada.

Yuan, B., Wang, W., Moghanloo, R.G., 2017. Permeability Reduction of Berea Cores Owing to Nanoparticle Adsorption onto the Pore Surface: mechanistic Modeling and Experimental Work. Energy Fuels 31 (1), 795–804. https://doi.org/10.1021/acs.energyfuels.6b02108.